Journal of Power Sources 226 (2013) 27–32

Contents lists available at SciVerse ScienceDirect

Journal of Power Sources

journal homepage: www.elsevier.com/locate/jpowsour

Short communication

An electrodeposited redox polymer–laccase composite film for highly efficient four-electron oxygen reduction

Wei Shen, Huimin Deng, Alan Kay Liang Teo, Zhiqiang Gao*

Department of Chemistry, National University of Singapore, Singapore 117543, Singapore

HIGHLIGHTS

- ► Thin films of redox polymer–laccase composite are electrodeposited onto carbon electrodes under mild conditions.
- ► The deposited films catalyze the electroreduction of O_2 at an operating potential of 0.58 V (vs. Ag/AgCl).
- ► The deposited films show excellent performance in terms of O_2 electroreduction current density and stability.

ARTICLE INFO

Article history:
Received 16 July 2012
Received in revised form
14 September 2012
Accepted 12 October 2012
Available online 29 October 2012

Keywords:
Oxygen
Laccase
Biofuel cell
Redox polymer
Electrocatalysis
Carbon electrode

ABSTRACT

In this report, it is shown that novel thin films of $Os(dcbpy)_2$ (dcbpy = 4,4′-dicarboxylic acid-2,2′-bipyridine)-based redox polymer–laccase composite can be electrodeposited onto carbon electrodes under mild conditions. In a nutshell, the exchange of the inner-sphere Cl^- of the $Os(dcbpy)_2Cl^{+/2+}$ complex tethered to partially quaternized poly (4-vinylpyridine) (PVP) by a pyridine ligand of a second PVP chain leads to cross-linking and deposition of the redox polymer. Laccase, which has coordinatively linkable functions of amines and histidines, is readily incorporated in the electrodeposited redox polymer. Because the reaction centers of the co-deposited laccase are electrically connected to the electrode through the deposited redox polymer, the electrodeposited film can catalyze the electroreduction of O_2 at 0.58 V (vs. Ag/AgCl) – the least reducing potential for highly efficient four-electron reduction of O_2 in pH 5.5 0.10 M phosphate buffer solution. Furthermore, the electroreduction of O_2 is found to be O_2 transport-limited when the reduction potential is poised at $\geq$120 mV more reducing than that of the reversible O_2/H_2O couple. This composite film could be an excellent candidate for uses as cathode in enzymatic biofuel cells.

1. Introduction

Biofuel cells convert the chemical energy of a biofuel into electrical energy by means of biochemical pathways [1–3]. A variety of approaches have been proposed in the operation of the biofuel cells [1–9]. In addition, a number of high energy density biofuels, such as methanol, ethanol, and sugars, have been tested in the biofuel cells. Amongst them, the glucose–O_2 enzymatic biofuel cells, where glucose is electrooxidized to gluconolactone at the anode and O_2 is electroreduced to water at the cathode, are the most studied [1–5,10–12]. Unlike other types of fuel cells, the enzymatic biofuel cells are expected to be operable under mild physiological conditions [6,12]. More importantly, they are highly miniaturizable because they can be operated in a compartmentless manner [13–15]. Although their energy conversion efficiencies are usually not as high as other biofuel/biomass-based energy conversion devices, the enzymatic biofuel cells can potentially be the energy sources of implanted biomedical devices since the biofuels, such as glucose and O_2 required for their operation, can feasibly be drawn from their immediate environment [15]. The first example of the enzymatic biofuel cells, employing glucose oxidase to oxidize glucose at the anode, was constructed in 1962 [16]. Although great progress has been made in the past 20 years, a number of challenges remain to be addressed. These include relatively short lifetime, low power output, and poor biocompatibility. For instance, most of the proposed enzymatic biofuel cells are capable of meeting the demands of implanted medical devices for short term applications of only up to days, whereas lifetime in the order of weeks, months, or even years would be required for powering implanted medical devices [1–5]. The low power output

* Corresponding author. Tel.: +65 6516 3887; fax: +65 6779 1691.
E-mail address: chmgaoz@nus.edu.sg (Z. Gao).

0378-7753/$ – see front matter © 2012 Elsevier B.V. All rights reserved.
http://dx.doi.org/10.1016/j.jpowsour.2012.10.031

is largely due to the fact that in most of the glucose–O_2 biofuel cells, the O_2 cathode is often the limiting factor in determining the current density due to the much lower concentration of O_2 in aqueous solutions and biological fluids. Besides, the turnover rates of the immobilized enzymes are normally lower than those found in their corresponding natural systems [17,18]. To address these problems, wired-enzyme technology, where a mediating species is chemically bound to a polymer backbone (redox polymer) and to the enzyme in a manner that allows close contact between the redox centers of the enzyme, has been developed. By bypassing the natural route, the redox polymer serves to "electronically wire" the enzyme to facilitate a free flow of electrons from the enzyme to the electrode via the mediator [5,19]. On the other hand, the direct adsorption of some enzymes, including laccase, onto the surface of an electrode without their "wiring" also allows flow of electrons [20,21]. Nonetheless, the transfer of electrons from the electrode to the adsorbed enzyme requires the orientation of the active sites of the enzyme to be toward the surface of the electrode. Since only a small fraction (<2%) of one monolayer of the randomly oriented enzyme is appropriately oriented, the current density that is reached does not approach that of the wired-enzyme electrode and this limits the practical value of the biofuel cells employing the adsorbed enzymes. The reason for the much higher current density for the former is that in the redox hydrogel, the enzyme does not need to orientate itself relative to the surface of the electrode; all reaction centers are wired to the electrode through the redox centers of the hydrogel in a three-dimensional manner with its mobile segments approaching the enzyme's reaction centers. Furthermore, not one layer, but multiple layers of enzyme in the three-dimensional volume of a hydrogel are brought into electrical contact with the electrode [19]. A number of enzyme electrodes and biofuel cells have been fabricated based on this technology [1–5]. Both the current density and stability of such devices have been improved substantially. However, an important consideration for the future development of the enzymatic biofuel cells is about developing new immobilization strategies that are appropriate for the construction of highly stable miniature biofuel cells which require the precise control of film deposition on spatially discrete electrode areas. Electrochemical immobilization provides an elegant alternative for the one-step deposition of enzymes on a small-area electrode of defined geometry [22–24]. Such immobilization provides a simple but versatile approach for controlling the amount and spatial distribution of the deposited film and is especially applicable to the construction of micrometer-size biofuel cells. To date, the majority of such studies have focused on the immobilization of enzyme in electrochemically generated conducting polymer matrixes. However, they could pose serious difficulties in practical applications since there is no direct electron transfer between the enzyme and the conducting polymer backbone. Hence, either a mediator or a high potential is needed to monitor the enzymatic reaction.

In this report, we focused on the immobilization and optimization of a laccase-mediator pair to function optimally as an O_2 reduction cathode for the enzymatic biofuel cells. A novel redox polymer containing osmium-4,4′-dicarboxylic acid-2,2′-bipyridine (dcbpy) complex was chosen as the electron mediator (wire). The redox polymer displayed good kinetics and excellent mediating power with respect to laccase. More importantly, this redox polymer and laccase can be electrochemically co-deposited onto a carbon electrode, thus forming an insoluble film with laccase on the carbon electrode via coordinative cross-linking. The resulting redox polymer–laccase composite film showed excellent performance in terms of O_2 electroreduction current density and stability, opening new perspectives for the enzymatic biofuel cells operating at higher current density with better stability.

2. Experimental section

2.1. Reagents and apparatus

$(NH_4)_2OsCl_6$, poly (4-vinylpyridine) (PVP) (M_w 60,000), and laccase were purchased form Sigma–Aldrich (St Louis, MO) and purified following a published procedure [25]. $Os(dcbpy)_2Cl_2$ was synthesized from $(NH_4)_2OsCl_6$ followed the procedure proposed by Lay and co-workers [26]. The redox polymer used in this work was partially quaternized PVP (QPVP) pyridine-complexed with $Os(dcbpy)_2Cl^{+/2+}$ (QPVP-Os). The quaternization is meant to increase its solubility in water and to maximize laccase loading through the formation of additional electrostatic adducts during electrodeposition. Synthesis of the polymer was described elsewhere [27]. The structure of the redox polymer is given in Fig. 1. A 0.10 M phosphate buffer solution was used as the supporting electrolyte for electrochemical tests. The pH of the phosphate buffer was adjusted by adding an appropriate amount of phosphoric acid or sodium hydroxide. All solutions were freshly prepared with ultrapure water and certified analytical reagents from Sigma–Aldrich.

Electrochemical experiments were carried out using a CH Instruments Model 760D electrochemical workstation (CH Instruments, Austin, TX). A three-electrode system, consisted of a carbon working electrode, a BAS micro-Ag/AgCl (KCl saturated) reference electrode (Bioanalytical System, Inc., West Lafayette, IN) and a platinum wire counter electrode, was used in all electrochemical experiments. An analytical rotator (Pine Instrument Company, Grove City, PA) was used to control convection processes when needed. Electrodeposition of the redox polymer–laccase composite film was performed in a home-made small volume (1.0 mL) electrochemical cell. All potentials reported were referred to the Ag/AgCl reference electrode.

2.2. Electrodeposition of redox polymer–laccase composite film on carbon electrode

The electrodeposition of the redox polymer–laccase composite film on a carbon electrode (glassy carbon, screen-printed carbon, wax-impregnated graphite, and carbon cloth) was carried out as previously described with slight modification [23]. Briefly, square waves between −0.2 and 1.2 V were applied to an O_2 plasma-treated carbon electrode in a pH 7.4 0.10 M phosphate buffer containing 1.0 mg mL^{-1} redox polymer and 2.0 mg mL^{-1} laccase under

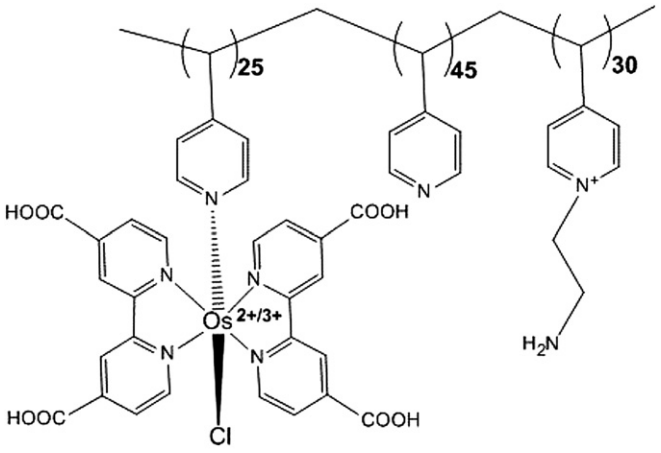

Fig. 1. Chemical structure of the redox polymer used in the preparation of the redox polymer–laccase composite film.

ambient conditions. After the electrode was removed from the depositing solution and thoroughly rinsed with water, it was dipped in the pH 7.4 phosphate buffer and treated with potential cycling between −0.2 and 0.8 V until a steady-state voltammogram was attained. Thick films could be deposited on the electrode by extending the number of the square waves. It has been shown that various functional groups such as hydroxyls and carbonyls are among the possible oxidation products on the carbon electrode surface [28]. It is likely that the carbonyl groups convert the neutral carbon electrode to a somewhat negatively charged one. Therefore, electrostatic interaction helps to attract and retain the redox polymer on the electrode surface and provides a high concentration of the redox polymer necessary for the electrodeposition.

3. Results and discussion

3.1. Electrochemistry of the redox polymer–laccase composite film

Fig. 2 shows the voltammograms of the redox processes of $Os(dcbpy)_2Cl_2$ complex and the QPVP-Os redox polymer in solution. Upon substitution of the inner-sphere Cl^- of $Os(dcbpy)_2Cl_2$ by the polymer-bound pyridine, the redox potential was shifted positively by about 100 mV. As discussed by Lever [29], the more strongly a ligand withdraws electrons and coordinates to the osmium ion, the greater is the positive shift of the redox potential. Thus, the 100 mV-shift is caused by the stronger electron withdraw property of the pyridine ligand. As seen in Fig. 2, the only obvious electrochemical process between −0.2 and +1.0 V is the reduction–oxidation of the Os(III)/Os(II) couple. Fig. 3 shows the steady-state voltammogram of the redox polymer–laccase composite film at 10 mV s^{-1} in a thoroughly deoxygenated 0.10 M pH 5.5 phosphate buffer at 37 °C. Its voltammogram is characteristic of a polymer-bound osmium complex with an apparent redox potential of +0.58 V. When a fresh redox polymer–laccase composite film was subjected to potential cycling, a pronounced tailing of the voltammogram was observed. With increasing number of potential cycles, this tailing gradually disappeared and a well-defined steady-state voltammogram was obtained. Thereafter, little change was observed during extended potential cycling up to 2 h. This behavior of the fresh film may be due to the reorganization of the redox centers in the film. As illustrated in Fig. 3, the redox polymer–laccase composite film exhibited exactly as expected for a highly reversible surface confined redox couple [30]. The width of the peaks at half-height was ~170 mV. This was much wider than the theoretical width of 90.6 mV for an ideal Nernstian one-electron-transfer reaction, indicating that there is considerable repulsive interaction in the film because of the high density of positive charges from the polymer backbones and the osmium redox pendants [31]. The peak currents were found to be linear with the potential scan rates up to 500 mV s^{-1} and the ratio of the anodic to the cathodic charge, obtained by integrating the current peaks at slow scan rates, was close to theoretical, showing that both the transport of electrons and counter-ions within the film were rapid [30]. Deviation from linearity, accompanied by a tailing current was observed only at very high scan rates and for thick films. The surface charge density, obtained by integrating either the reduction or the oxidation peak, gave similar values of 3.8×10^{-10} to 2.1×10^{-8} mol cm^{-2} for the electroactive centers on the electrode surface. The corresponding film thickness, determined by field emission scanning electron microscopy, was in the range of 6.0–540 nm. When the number of the applied square waves was less than 200, there was a linear correlation between the film thickness and the number of the applied square waves. The presence of laccase in the film did not appreciably alter the electrochemistry of the redox polymer. At low scan rates, the two waves almost mirrored each other; the separations of their peak potentials (ΔEp) were less than 10 mV and close to the nil-value characteristic of a strongly adsorbed reversible redox couple [30]. This much smaller ΔEp is another indication that the electron-transfer rate within the film and the electron exchange rate between the film and the substrate electrode is very fast and this paves the way for the development of a highly efficient cathode for the enzymatic biofuel cells. On the contrary, in the much thicker solvent-cast and chemically cross-linked films, the peaks of the reduction and oxidation branches of the voltammogram were separated by >50 mV [32,33]. Furthermore, excellent mechanical strength of the deposited film was observed and this is attributed to the electrochemical crossing-linking, akin to that of polymer-based plastic materials by cross-linking through covalent bonds.

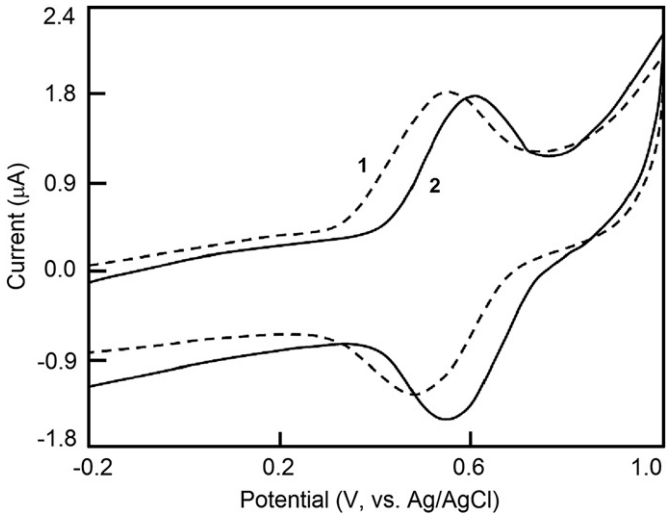

Fig. 2. The cyclic voltammograms of (1) 0.50 mg mL^{-1} $Os(dcbpy)_2Cl_2$ and (2) 2.5 mg mL^{-1} QPVP-Os. 3-mm Diameter glassy carbon electrode in pH 7.0 0.10 M phosphate buffer, potential scan rate 100 mV s^{-1}.

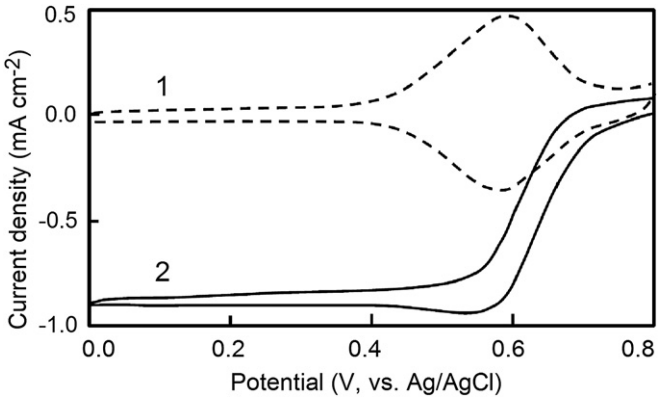

Fig. 3. The cyclic voltammograms at 10 mV s^{-1} of the QPVP-Os–laccase film coated carbon electrode in (1) deoxygenated and (2) oxygenated pH 5.5 0.10 M phosphate buffer.

3.2. Electrocatalytic reduction of O_2

As demonstrated in previous reports, the reduction of O_2 is mediated by the osmium–bipyridine complex-based redox polymers [32–34]. Upon oxygenation of the phosphate buffer at 1.0 O_2 atm, a typical catalytic reduction wave was obtained and the

oxidation peak of the redox polymer was completely eliminated (Fig. 3), indicating a highly efficient catalytic reaction [30]. The redox-active Os(II)/(III) moieties in the deposited film act as artificial electron donors in place of phenolic compounds for laccase and electron shuttles between the substrate electrode and laccase, as illustrated in Scheme 1. The electroreduction of O_2 commenced at ~0.70 V (the redox potential of the reversible O_2/H_2O couple at pH 5.5) and reached its maximum at 0.58 V, the most anodic O_2 reduction potential amongst enzymatically catalyzed O_2 electroreduction [1–3]. The absence of the oxidation wave in the voltammogram at this scan rate (10 mV s^{-1}) showed that the film is homogeneously maintained in the reduction state by the transfer of electrons from the redox centers of laccase to the Os(III) complex in the redox polymer. Supportive evidence was found from the very low hysteresis between the forward and the reverse scan. In addition, the reproducibility of the O_2 electroreduction current was found to be >90% among the films from different batches.

Unlike the homogeneous solution reaction, the laccase-catalyzed O_2 electroreduction is highly localized; it only occurs at the redox polymer–laccase composite film on the electrode. As the four-electron laccase-catalyzed reduction of O_2 involves a cascade of events and several intermediates including H_2O_2 and $O^{2-\cdot}$ [35,36], these intermediates might diffuse away from the electrode before being reduced to the final product water. The "production" of the intermediates might compete with the desired four-electron reduction. The possibility of the intermediate production was tested using a rotating ring and disk electrode having an inner redox polymer–laccase composite film coated glassy carbon disk electrode and an outer platinum ring electrode. If H_2O_2 and $O^{2-\cdot}$ were produced on the coated glassy carbon disk electrode, it would have been detected at the platinum ring poised at 1.0 V; the H_2O_2 and $O^{2-\cdot}$ being electrooxidized to O_2 at the platinum ring at this potential. When O_2 was reduced on the glassy carbon disk electrode at increasing current densities from 1.0 to 10 mA cm^{-2}, only negligible current was detected at the platinum ring electrode and it remained unchanged throughout the experiment, suggesting that neither H_2O_2 nor $O^{2-\cdot}$ is produced in the laccase-catalyzed four-electron O_2 electroreduction. Moreover, after 10 h of O_2 electroreduction at 2.0 mA, the presence of H_2O_2 in the 10 mL phosphate buffer was tested with a standard colorimetric 3,3′,5,5′-tetramethylbenzidine-horseradish peroxidase (TMB-HRP) method [37]. H_2O_2 was not detected at >1.0 μM, the detection limit of the TMB-HRP method.

3.3. Optimization

The optimal composition of the depositing solution was determined for electrodes rotating at 2500 rpm and potential poised at 0.58 V. Fig. 4A shows the dependence of the deposition of the redox polymer–laccase composite film on the concentration of the redox polymer in the depositing solution. Good deposition of the composite film was observed through the 0.75–2.5 mg mL^{-1} range. Therefore, the polymer concentration was fixed at 1.0 mg mL^{-1} for the co-deposition of the redox polymer and laccase. As shown in Fig. 4A, the concentration of laccase in the depositing solution also has a profound effect on the electroreduction of O_2. From 0.10 to 0.50 mg mL^{-1}, the current density increased with the weight percentage of laccase, reaching 6.2 mA cm^{-2} in the range of 0.50–2.0 mg mL^{-1}. Above 2.0 mg mL^{-1}, the current density declined sharply and some precipitate in the depositing solution appeared when >3.0 mg mL^{-1} laccase was used. The precipitation is likely due to the formation of neutral electrostatic adducts between the anionic laccase and the cationic redox polymer in the pH 7.4 phosphate buffer.

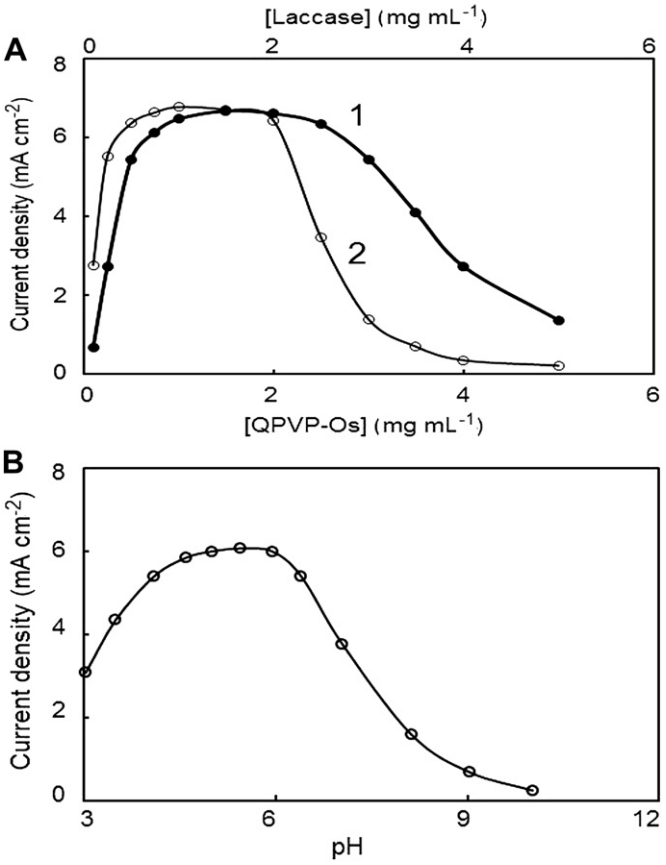

Fig. 4. (A) The dependence of the O_2 electroreduction current density on (1) the concentration of QPVP-Os (laccase concentration was fixed at 2.0 mg mL^{-1}) and (2) laccase (QPVP-Os concentration was fixed at 1.0 mg mL^{-1}). (B) The effect of solution pH on the electroreduction current density of O_2 of the redox polymer–laccase composite film. 1 atm O_2 in the pH 5.5 phosphate buffer at 37 °C, poised potential 0.58 V.

The effect of pH on the electroreduction current density of O_2 was also studied in the phosphate buffer for the electrode rotating at 2500 rpm and its potential poised at 0.58 V. The pH values of the phosphate buffer were adjusted by adding appropriate amounts of 0.10 M phosphoric acid and sodium hydroxide as needed, respectively. As shown in Fig. 4B, the current density increased with increasing pH from 3.0 to 5.0, plateaued in the range of 5.0–6.0, and then declined precipitately above pH 6.0. There was no irreversible change in the current characteristics between pH 3.0 and 8.0; below pH 3.0 and above pH 10, the electrode was irreversibly damaged quickly. Practically, there was no difference in the maximum current density attained when 0.10 M pH 5.5 phosphate, acetate, or citrate buffer was used.

The energy level of the electron in the carbon electrode is exclusively determined by the potential applied to it. When a sufficiently reducing potential is applied, the electron exchange

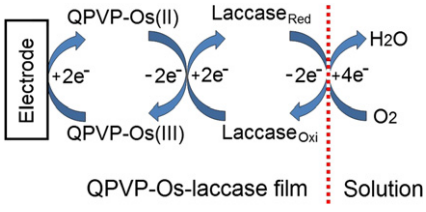

Scheme 1. Illustration of the catalytic reduction of O_2 at the QPVP-Os–laccase film coated electrode.

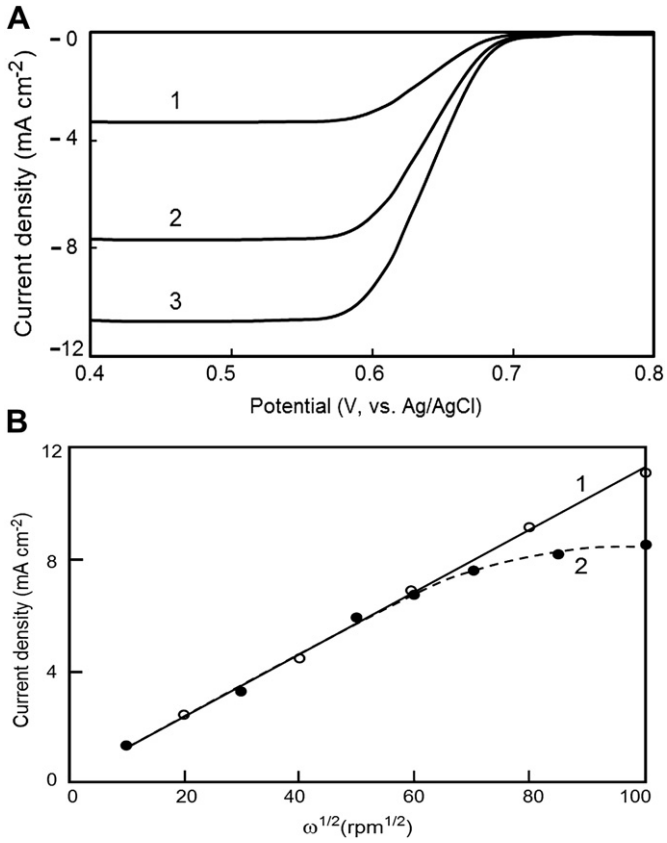

Fig. 5. (A) The electroreduction of O_2 at the electrodeposited redox polymer–laccase composite film coated carbon electrode rotating at (1) 1000, (2) 5000, and (3) 10,000 rpm. (B) Levich plots for rotating electrodes coated with (1) the electrodeposited and (2) the chemically cross-linked redox polymer–laccase films, respectively. 1 atm O_2 in the pH 5.5 phosphate buffer at 37 °C, poised potential 0.58 V.

rate at the redox polymer–laccase film/carbon electrode interface is very rapid and it can never be the rate-limiting step. Therefore, the rate-limiting step(s) must be one of the following: (1) catalytic process at the film–solution interface, (2) charge transfer process within the film, or (3) mass-transport process in the solution. If the electroreduction of O_2 is controlled solely by the mass-transport process in the solution, the relationship between the limiting current (i_L) and the rotating speed of the electrode should obey the Levich equation [30]:

$$i_L = 0.620nFAD^{2/3}\nu^{-1/6}\omega^2 C \quad (1)$$

where D, ν, ω and C, are respectively the diffusion coefficient, the kinetic viscosity, the rotating speed of the electrode and the bulk concentration of the reactant in solution. The other symbols have their usual meanings. According to the Levich equation (1), the plot of the limiting current density i_L as a function of $\omega^{1/2}$ should be a straight line. Fig. 5B shows the dependence of i_L on $\omega^{1/2}$ of the rotating electrode up to the upper limit of 10,000 rpm of the rotator with a current density of ~11 mA cm^{-2} (the highest among the reported values for the enzyme-catalyzed electroreduction of O_2 [1–3]). Indeed, i_L increased linearly with $\omega^{1/2}$, in accordance with the Levich equation (1), indicating that the charge transfer process is very fast. The deposited film has excellent catalytic power for the electroreduction of O_2 and the O_2 electroreduction process is entirely controlled by the transport of O_2 in solution under 1 atm O_2 when the electrode was poised at potential ≤ 0.58 V (≥120 mV more reducing than that of the reversible O_2/H_2O couple). Unfortunately, the low concentration of O_2 prevented us from looking at the effects of the other two processes. This excellent catalytic power of the redox polymer–laccase composite film at the least reducing potential is probably attributed to the high $Os(dcbpy)_2^{2+/3+}$ loading (25%) and the absence of a cross-linking agent which produces the highest possible density of the osmium redox centers for highly efficient conduction of electrons. In contrast, when the chemically cross-linked redox polymer–laccase composite film was tested under the same conditions, the current density continued to increase with $\omega^{1/2}$, but no longer linearly for $\omega > 4000$ rpm, until it reached the kinetic limit of ~9.2 mA cm^{-2}. Now, the O_2 electroreduction is limited by the electron-transfer process within the redox hydrogel film. Similar observations have been reported [38,39]. Continuous testing of the rotating electrode at 2500 rpm for 24 h showed little loss due to wear and tear. Moreover, the redox polymer composite film showed no loss of its catalytic power after six months of dry storage at −20 °C. On the other hand, unlike the bilirubin oxidase-based catalytic systems [11,39–41], besides the pronounced effect from pH as discussed above, chloride was found to poison the composite film. For example, the current density declined by ~38% when 0.15 M chloride was added to the pH 5.5 0.10 M phosphate buffer.

4. Conclusion

The experimental results reported herein demonstrate the feasibility of fabricating an O_2 cathode by electrochemically co-depositing the osmium containing redox polymer–laccase composite film onto carbon electrode under mild conditions. Since the deposition is only restricted to the electrode surface, it is an effective procedure for the selective deposition of the composite film and incorporation to microbiofuel cells. The co-deposition of laccase in the redox polymer leads to electrical wiring of the enzyme and the formation of an O_2 electroreduction catalyst. The osmium complex in the composite film efficiently mediates the electron transfer from laccase to the substrate electrode, thus allowing the four-electron reduction of O_2 to water at a current density as high as 11 mA cm^{-2} with good stability. The application of the developed O_2 cathode in biofuel cells is currently underway.

Acknowledgments

This work is supported by Agency for Science, Technology and Research (A*STAR) Singapore through the A*STAR-ANR Program.

References

[1] S.C. Barton, J. Gallaway, P. Atanassov, Chem. Rev. 104 (2004) 4867–4886.
[2] M. Zhou, S.J. Dong, Acc. Chem. Res. 44 (2011) 1232–1243.
[3] R.A. Bullen, T.C. Arnot, J.B. Lakemanc, F.C. Walsh, Biosens. Bioelectron. 21 (2006) 2015–2045.
[4] F. Gao, L. Viry, M. Maugey, P. Poulin, N. Mano, Nat. Commun. 1 (2010). Art. no. 2.
[5] A. Heller, Phys. Chem. Chem. Phys. 6 (2004) 209–216.
[6] E. Katz, A.N. Shipway, I. Willner, in: W. Vielstich, H.A. Gasteiger, A. Lamm (Eds.), Handbook of Fuel Cells-Fundamentals, Technology and Applications, Fundamentals and Survey of Systems, vol. 1, John Wiley & Sons, Hoboken, NJ, 2003, pp. 355–381.
[7] F. Mao, N. Mano, A. Heller, J. Am. Chem. Soc. 125 (2003) 4951–4957.
[8] C.F. Meunier, Y.Y. Xiao, J.C. Rooke, B.L. Su, ChemCatChem 3 (2011) 476–488.
[9] G.T.R. Palmore, G.M. Whitesides, in: E. Himmel (Ed.), Enzymatic Conversion of Biomass for Fuels Production, vol. 566, American Chemical Society, 1994, pp. 271–290.
[10] N. Mano, F. Mao, A. Heller, J. Am. Chem. Soc. 124 (2002) 12962–12963.
[11] N. Mano, F. Mao, A. Heller, J. Am. Chem. Soc. 125 (2003) 6588–6594.
[12] I. Willner, Y.M. Yan, B. Willner, R. Tel-Vered, Fuel Cells 9 (2009) 7–24.
[13] T. Chen, S.C. Barton, G. Binyamin, Z.Q. Gao, Y.C. Zhang, H.H. Kim, A. Heller, J. Am. Chem. Soc. 123 (2001) 8630–8631.
[14] E. Katz, I. Willner, A.B. Kotlyar, J. Electroanal. Chem. 479 (1999) 64–68.
[15] L. Halámková, J. Halamek, V. Bocharova, A. Szczupak, L. Alfonta, E. Katz, J. Am. Chem. Soc. 134 (2012) 5040–5043.

[16] J.B. Davis, H.F. Yarbrough, Science 137 (1962) 615–616.
[17] Y. Yan, O. Yehezkeli, I. Willner, Chem. Eur. J. 13 (2007) 10168–10175.
[18] X.Y. Zhao, H.F. Jia, J. Kim, Biotechnol. Bioeng. 104 (2009) 1068–1074.
[19] A. Heller, Acc. Chem. Res. 23 (1990) 128–134.
[20] S. Rubenwolf, O. Strohmeier, A. Kloke, S. Kerzenmacher, R. Zengerle, F. Von Stetten, Biosens. Bioelectron. 26 (2010) 841–845.
[21] M.R. Tarasevich, A.I. Ymopolov, V.A. Bogdanovskaya, S.D. Varfolojieev, Bioelectrochem. Bioenerg. 6 (1979) 393–403.
[22] N.C. Foulds, C.R. Lowe, Anal. Chem. 60 (1988) 2473–2478.
[23] Z.Q. Gao, G. Binyamin, H.H. Kim, S.C. Barton, Y.C. Zhang, A. Heller, Angew. Chem. Int. Ed. 41 (2002) 810–813.
[24] S.E. Wolowacz, B.F.Y. Yon-Hon, C.R. Lowe, Anal. Chem. 64 (1992) 1541–1545.
[25] N.S. Hudak, S.C. Barton, J. Electrochem. Soc. 152 (2005) A876–A881.
[26] P.A. Lay, A.M. Sargeson, H. Taube, Inorg. Synth. 24 (1986) 291–306.
[27] A. Aoki, R. Rajagopalan, A. Heller, J. Phys. Chem. 99 (1995) 5102–5110.
[28] D.M. Anjo, M. Kahr, M.M. Khodabakhsh, S. Nowinski, M. Wanger, Anal. Chem. 61 (1989) 2603–2608.
[29] A.B.P. Lever, Inorg. Chem. 29 (1990) 1271–1285.
[30] A.J. Bard, L.R. Faulkner, Electrochemical Methods: Fundamentals and Applications, John Wiley and Sons, New York, 2001.
[31] J.R. Lenhard, R.W. Murray, J. Am. Chem. Soc. 100 (1978) 7870–7875.
[32] S.C. Barton, M. Pickard, R. Vazquez-Duhalt, A. Heller, Biosens. Bioelectron. 17 (2002) 1071–1074.
[33] N. Mano, V. Soukharev, A. Heller, J. Phys. Chem. B 110 (2006) 11180–11187.
[34] S.C. Barton, H. Kim, G. Binyamin, Y. Zhang, A. Heller, J. Am. Chem. Soc. 123 (2001) 5802–5803.
[35] F. Guillen, C. Munoz, V. Gomez-Toribio, A.T. Martinez, M.J. Martinez, Appl. Environ. Microbiol. 66 (2000) 170–175.
[36] A.W. Tepper, S. Milikisyants, S. Sottini, E. Vijgenboom, E.J.J. Groenen, G.W. Canters, J. Am. Chem. Soc. 131 (2009) 11680–11682.
[37] P.D. Josephy, T. Eling, R.P. Mason, J. Biol. Chem. 257 (1982) 3669–3675.
[38] S.C. Barton, H. Kim, G. Binyamin, Y. Zhang, A. Heller, J. Phys. Chem. B 105 (2001) 11917–11921.
[39] N. Mano, H. Kim, Y. Zhang, A. Heller, J. Am. Chem. Soc. 124 (2002) 6480–6486.
[40] F. Durand, C.H. Kjaergaard, E. Suraniti, S. Gounel, R.G. Hadt, E.I. Solomon, N. Mano, Biosens. Bioelectron. 35 (2012) 140–146.
[41] N. Mano, H.H. Kim, A. Heller, J. Phys. Chem. B 106 (2002) 8842–8848.